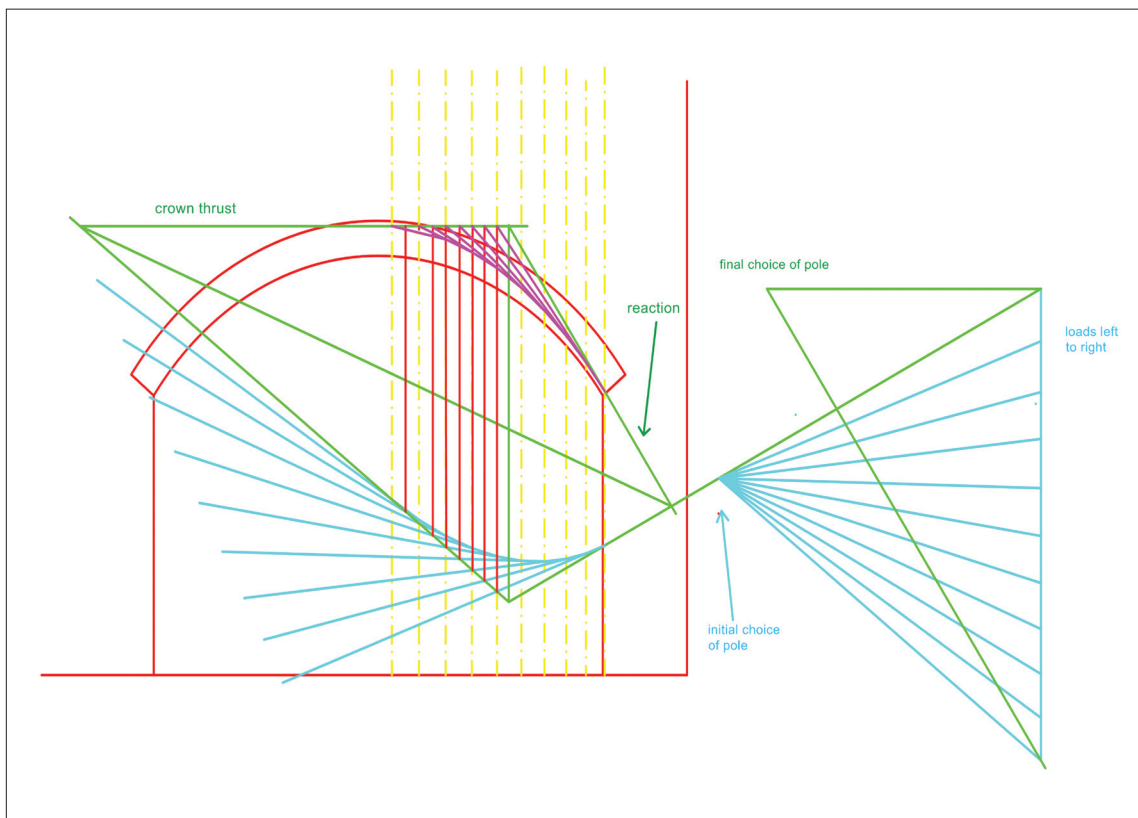


## Analysis of Segmental and Semicircular Masonry Arches

THOMAS E. BOOTHBY



**Fig. 1.**

*Illustrative application of graphical analysis for a symmetrical half-arch. The red lines represent the outlines of the arch and abutment. The dashed yellow lines represent lines of action of weight segments of the arch ring. Cyan lines represent initial choice of pole and construction of the funicular polygon. Green lines represent construction of resultant of load on half-arch, reaction, and crown thrust. Magenta lines represent construction of final thrust line. Figure by Karissa Shaner.*

A masonry arch is an assembly of wedges made of stone or brick that form a regular curve to support wall loads above an opening. An arch redirects gravity load to the supports of the arch. As this load is redirected, horizontal forces develop at the supports, in addition to the vertical forces due to gravity. This *Practice Point* reviews the failure modes that may occur in an arch in a building and the empirical, analytical, and graphical methods for determining the susceptibility of the arch to these types of failure. An extended example will show the application of these analysis methods. Figure 1 shows

the results of a computer analysis of an example arch. This procedure will be explained below, and other methods of arch assessment will be similarly described.

### Arch Dimensions

Five principal dimensions characterize the proportions of a segmental arch: span, rise, ring thickness, intrados radius, and angle of embrace. The following geometrical formulas can be used to convert quantities among span, rise, radius, and angle of embrace.<sup>1</sup>

$$S = 2r \sin \beta/2$$

$$R = r (1 - \cos \beta/2)$$

$$r = \frac{(R^2 + (S/2)^2)}{2R}$$

$$\beta = 2 \sin^{-1} (S/2r)$$

In these equations, span is abbreviated as  $S$ , rise as  $R$ , radius as  $r$ , and angle of embrace as  $\beta$ . Figure 2 shows a typical building arch, where the principal parts and the dimensions used in the formulas above are labeled.

**Fig. 2.** Residence, State College, Pennsylvania, date unknown, north elevation, showing detail of typical arch. The span is approximately 80 inches, the rise is 8 inches, and the thickness is 8 inches. The arch is understrength by the empirical rule, having a span:thickness ratio of approximately 10, which is greater than the minimum prescribed ratio of 6. All photographs by author, 2020, unless otherwise stated.

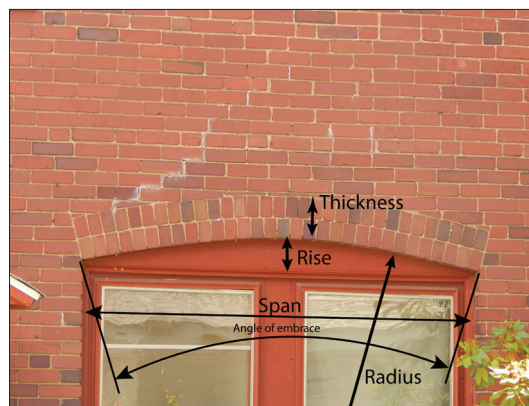


**Fig. 3.** Centre County Law Library, Bellefonte, Pennsylvania, ca. 1920, south elevation, showing abutment yielding in a flat arch. A triangular wedge of masonry has dislodged from above the arch as the arch settles.



**Fig. 4.** Centre County Law Library, south elevation, showing unsymmetrical failure of a building arch.



## Forms of Arch Failure

The purpose of analyzing an arch is to determine the potential failure modes and the susceptibility of the arch to these weaknesses. It is, therefore, worthwhile to review the types of failure that may occur in an arch: support settlement, support yielding, hinging of the arch, or material failure. The most common forms of failure involve the abutments or supports of the arch. Simple failure of the arch ring without the involvement of the supports is uncommon for an arch that meets the empirical ratios described below.

The common types of abutment failures are settlement and yielding. Differential settlement between the two supports produces asymmetrical damage in the arch and can often be diagnosed by the irregular appearance of the damage to the left and right of the centerline of the arch. Yielding, or horizontal movement of the abutment, occurs especially in flat arches, where the horizontal thrust is greater. Due to the geometry of a low-rise arch, the arch ring is very susceptible to sagging in the presence of this type of failure. Abutment yielding is a very common failure mode in brick facades and can be diagnosed by the partial separation of a triangular wedge of bricks above a low-rise arch (Fig. 3). Vertical settlement of one of the supports, on the other hand, produces an asymmetrical pattern of damage (Fig. 4).

## Empirical Arch Assessment

Empirical analysis is an effective tool in the initial diagnosis of problems in masonry arches. In empirical analysis, the only factors considered are the proportions of the arch and the proportions of its abutment. Loads, material properties, and other engineering attributes are omitted from this method, except that different proportional ratios may apply for different materials. Most existing arches in buildings were designed using proportional rules or some sense of proper proportioning. Appropriate proportions for arches depend on the span:rise ratio, with thinner arch rings allowed for lesser span:rise ratios. For a semicircular arch (where the span:rise ratio equals 2), the span:thickness ratio of the arch should be less than 20, whereas, for a flat arch (where the span:rise ratio is theoretically infinite), a span:thickness ratio of 6 to 8 is more sensible.

Since this *Practice Point* covers primarily the assessment of existing arches, the proportional ratios presented here are useful for a preliminary assessment of an existing arch. When the recommended span:thickness ratios are exceeded, it becomes important to complete a more detailed analysis. In ad-

## Terminology

**Abutment** | The support of the arch, offering horizontal and vertical force resistance. The width of the abutment is measured from the intrados at the skewback to the edge of the wall supporting the arch.

**Angle of embrace** | The angle between the mortar beds at the intrados at the two springing line points.

**Arch ring** | The portion of the arch with radial joints.

**Eccentricity** | The difference between the center of pressure within the arch ring and the physical centerline.

**Extrados** | The outer face of the arch ring.

**Intrados** | The inner face of the arch ring.

**Jack arch or flat arch** | An arch with horizontal intrados and extrados and with joints that radiate from a center.

**Keystone** | The center or highest voussoir.

**Pier** | An interior support for two adjacent arches.

**Ring thickness** | The distance from the intrados to extrados.

**Rise** | The height from the springing line at the intrados to the highest point of the intrados.

**Segmental arch** | An arch in the shape of a circular arc with a span:rise ratio greater than two.

**Skewback** | The inclined surface or joint upon which the end of the arch rests.

**Span** | The horizontal distance from the interior face of the abutment or the pier to the inner face of the adjacent abutment or pier.

**Spandrel** | The portion of the wall over the arch ring.

**Springer** | The lowest voussoir that rests on the abutment or pier.

**Springing line** | The inner edge of the skewback, which is the support point of the arch.

**Thrust line** | A line representing the location of the eccentric internal force in the arch.

**Voussoir** | In stone masonry arches, a single wedge-shaped stone.

dition to using empirical analysis as a screening measure, obvious settlement of the arch or its abutments or the appearance of large cracks (more than 5 millimeters) are also indications that a more detailed analysis may be required. The author has previously recommended an empirical rule for the assessment of the span:thickness ratio for an arch<sup>2</sup>:

$$S/t \leq 40r/S$$

where  $S$  is the span;  $t$  is the ring thickness; and  $r$  is rise of the arch. Thus, when  $r = 0.5S$  (semicircular arch),  $S/t \leq 20$  and when  $r \leq 0.25S$  (low-rise arch),  $S/t \leq 10$ .

This formula can also be applied to a flat arch. Although such an arch has no measurable rise, it does have an “implied rise” approximately equal to the thickness of the arch. Thus, substituting  $t$  for  $r$  in the above formula, one obtains  $S/t \approx 6$ , which is both a useful span:thickness ratio for a flat arch and a limit to the application of the above formula (Fig. 5).

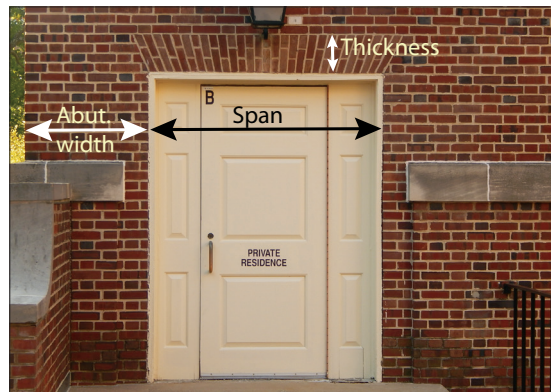


**Fig. 5.** Jordan Hall, University Park, Pennsylvania, ca. 1921, north elevation, showing a typical flat arch. The span:depth ratio is approximately 6.

The width of an abutment, measured in the span direction of the arch, is also a critical quantity.<sup>3</sup> A line from the extrados at the one-third point of the span to the intrados at the springing line, extended into the abutment, should be contained within the width of the abutment.

### Analytical Arch Assessment

Most analysis methods for an arch consist of determining the eccentricity of the internal axial force in the arch. Any loaded arch has a combination of axial force, shear, and bending moment at any section through the arch. The shear is insignificant for the assessment of the arch, but the relationship between the axial force and bending moment is critical. The net axial force is always compressive. The resistance of an arch to bending increases in the presence of axial force.<sup>4</sup>

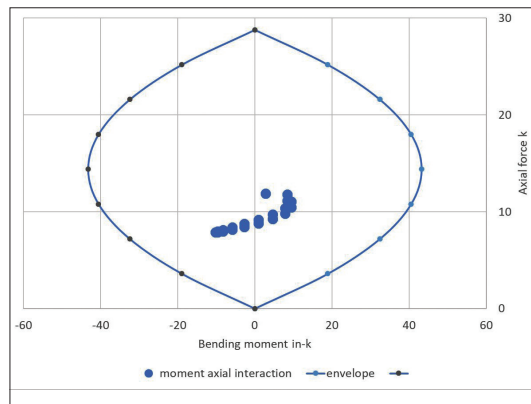
This *Practice Point* considers primarily the use of computer frame-analysis programs for the explicit analytical assessment of an arch. In such analysis, the arch is divided into segments along the centerline of the arch section. The computer program determines the internal force and moment at each subdivision point along the arch. In the output from any frame-analysis program, it is possible to determine the axial force, which acts along the centerline of the arch and combines with a bending moment  $M$ . The concentric  $P$  and  $M$  can be transformed to a force applied at an eccentricity of  $M/P$ , that is:

$$P_e = P_c \text{ and } P_e e = M$$

where  $P_e$  is the eccentric internal force;  $P_c$  is the concentric internal force;  $e$  is the eccentricity, which equals  $M/P$ ; and  $M$  is the bending moment.

The eccentricity, measured from the geometric center of the arch ring, is a very useful value because, for an arch with no resistance to tensile stresses (the usual assumption for masonry arches), the eccentricity has to be less than half the thickness of the arch. A limiting ratio as small as one-sixth may be considered, although the adoption of the one-sixth limit, known as the “middle-third rule,” may be unnecessarily conservative. This widely diffused middle-third rule is based on the assumption that the appearance of tension at the intrados or extrados precipitates failure of the arch. In fact, any portion of the arch can resist a compressive force centered very close to the intrados or extrados, nearly one-half the depth of the arch, without any threat to the stability of the arch.<sup>5</sup>

**Fig. 6.** Interaction diagram for a masonry arch. The envelope shows the maximum combinations of bending moment and axial force for an allowable compressive stress of 200 pounds per square inch. The points within the envelope represent the combinations of these forces calculated for the example arch in the final section of this article.



**Treatment of concentrated loads.** Concentrated loads on an arch are usually applied to the masonry wall above the arch. It is reasonable to assume that a concentrated load disperses through solid ashlar masonry at a ratio of one vertical to one horizontal

and for other materials at a ratio of two vertical to one horizontal.<sup>6</sup> For a concentrated load  $P$  at a height  $h$  above the extrados of the arch, the uniformly distributed load  $w$  is

$$w = P/kh \text{ distributed over a length } kh$$

where  $k$  equals two for solid ashlar masonry, and  $k$  equals one for brickwork. Thus, a 1,000-pound load applied 2 feet above a brick arch is applied to the arch as 500 pounds per foot over a length of 2 feet.

**Elastic analysis.** The elastic analysis of an arch is complicated by the curvature of the arch; by the rigidity of the supports, which make the arch three degrees statically indeterminate; and by the cracking of the arch, which causes the stiffness of the arch to be variable along its length. These difficulties render it very time-consuming to complete an elastic analysis of an arch using hand calculations. Reasonable results can be obtained using any frame-analysis program by dividing the length of the arch centerline into 10 or more segments and applying appropriate loads.

Reviewing the internal force output of the frame elements used in analysis, the eccentricity of the internal force can be determined at any point along the arch and compared to the thickness of the arch. It is useful to make a scatter plot of the axial force and moment results and compare them to a failure envelope. The failure envelope is a plot of the maximum combinations of axial force and bending moment (much like the interaction diagram for a reinforced-concrete column).<sup>7</sup> The simplest form of equation for this failure envelope, based on zero tensile capacity, is:

$$\frac{1}{4} \left| \frac{M}{M_0} \right| - \left( \frac{P}{P_0} \right) + \left( \frac{P}{P_0} \right)^2 \leq 0$$

$$P_0 = bhF_m$$

$$M_0 = \frac{1}{4} bh^2 F_m$$

where  $M$  is the calculated bending moment;  $M_0$  is the maximum bending moment in the absence of axial force;  $P$  is the calculated axial force;  $P_0$  is the maximum axial force in the absence of the bending moment;  $b$  is the width of the section of arch ring;  $h$  is the thickness of the arch ring; and  $F_m$  is the maximum allowable compressive stress in the masonry.

An example of such an interaction diagram is shown in Figure 6, along with the interaction points for arch analysis in the last section of this paper.

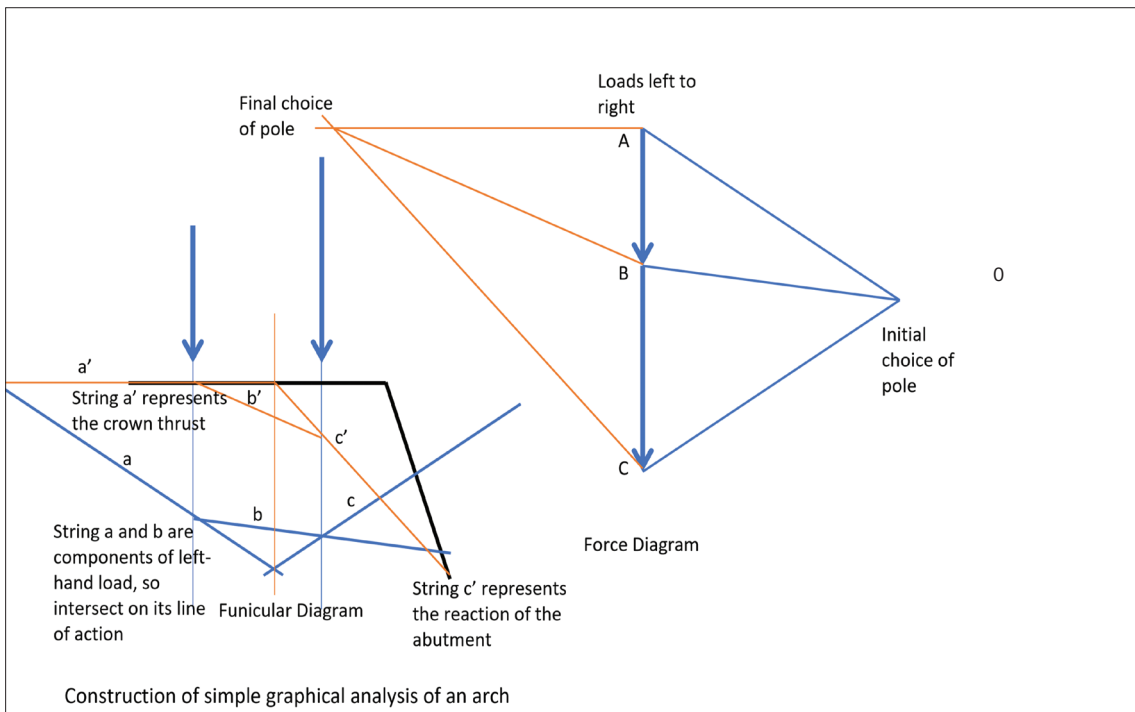


**Fig. 7.** Simplified application of graphical analysis for a symmetrical half-arch. Figure by Karissa Shaner.

**Plastic analysis.** The plastic analysis of arches was originally fully described by Jacques Heyman, who determined that the behavior of a joint in a masonry arch subjected to combined axial force and bending moment observed the laws of engineering plasticity.<sup>8</sup> This result can be expressed in two basic theorems. The upper-bound condition has been modified from its usual statement to describe the assessment of existing arches.

- Lower bound: If a statically admissible distribution of internal forces can be found for which the eccentricity is less than half the thickness, the arch is stable.
- Upper bound: If a kinematically admissible mechanism that causes net-negative virtual work can be found for a given load, then the arch is unstable.

Since the failure of a uniformly loaded arch due to distributed loads is rare, a very useful extension of these ideas to bounds on the load causing yielding failure at an abutment is available.<sup>9</sup> An example calculation of the lower bound and upper bound to the collapse load on an arch is shown in the example below.

**Graphical analysis.** Graphical methods are a very convenient way to determine the internal forces in an arch.<sup>10</sup> Using diagrams of the loads, internal forces, and locations within the arch, it is possible to use a geometrical construction to find the thrust line

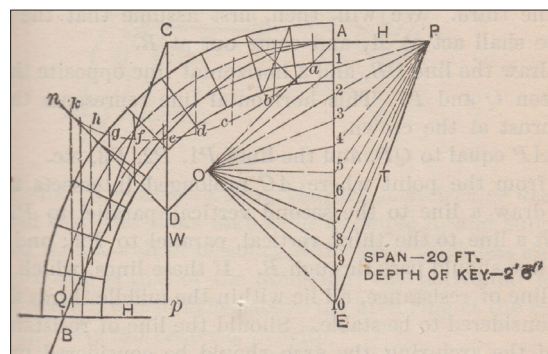


**Fig. 8.** Frank Kidder's construction of thrust line for a symmetrically loaded semicircular arch from *The Architect's and Engineer's Pocket Book*, 3rd ed. (New York: John Wiley and Sons, 1886).

and the internal forces and moments in the arch. Since an arch with fixed supports is three degrees statically indeterminate, a graphical construction of the internal forces provides a statically admissible distribution of internal forces, which verifies the lower-bound condition in plastic analysis. This topic will be considered below.

The graphical determination of the internal-force diagram of an arch uses two different constructions. The first, known as the force polygon, is a graphical solution of force equilibrium for the arch. The second, known as the funicular polygon, is a graphical solution of the location of all the internal forces in the arch. Figure 7 illustrates a very simplified version of the construction of the force and funicular polygons for two loads on a half-arch, plus the crown thrust and the reaction. Figure 8 illustrates the appli-

cation of this construction to a symmetrically loaded semicircular arch.<sup>11</sup> The force polygon graphically represents the equilibrium of the loads on the structure with the support reaction and the crown thrust. The magnitude and direction of the loads are considered in the force diagram by drawing vectors having the magnitude of the force for length and having the same direction at the force (the two forces A and C in Figure 7 and forces A1 through 10 in Figure 8).

The funicular polygon is a separate diagram that depicts the lines of action of the forces in the plane. By choosing an arbitrary point O, known as the pole, on the force diagram, each of the forces on the funicular diagram can be represented by two components, which must intersect on the line of action of the force. Thus, force AB on the force polygon in Figure 7 is represented by a line parallel to OA and a line parallel to OB, which intersect at some location on the line of action of the force AB in the funicular diagram on the left. This diagram is constructed sequentially through all of the forces under consideration (line segments a through n in Figure 8). The intersection of the first and last string is a point on the line of action of the resultant force. Thus, line CD in Figure 8 passes through the intersection of segment a and segment n and represents the resultant force of A1 through 10.

The thrust line within an arch may now be constructed. The crown thrust, a horizontal line beginning at point A in Figure 8, intersects line CD in C. The line of action of the support reaction passes through C

and through an arbitrary point at the base of the arch B. The slope of BC can be carried back to the force diagram to locate the final pole location (P in Figure 8). The remainder of the segments of the thrust line can be constructed using this pole location.

Uniformly distributed loads are simplified, dividing into a series of concentrated loads and operating on the concentrated loads in the manner described above.

**Combined graphical and elastic analysis.** Consistent with the above discussion, a thrust line can be plotted, and the forces can be read off the force polygon and transformed to axial force and eccentricity. These values can then be compared to a graphical failure envelope for the cross section of the arch.

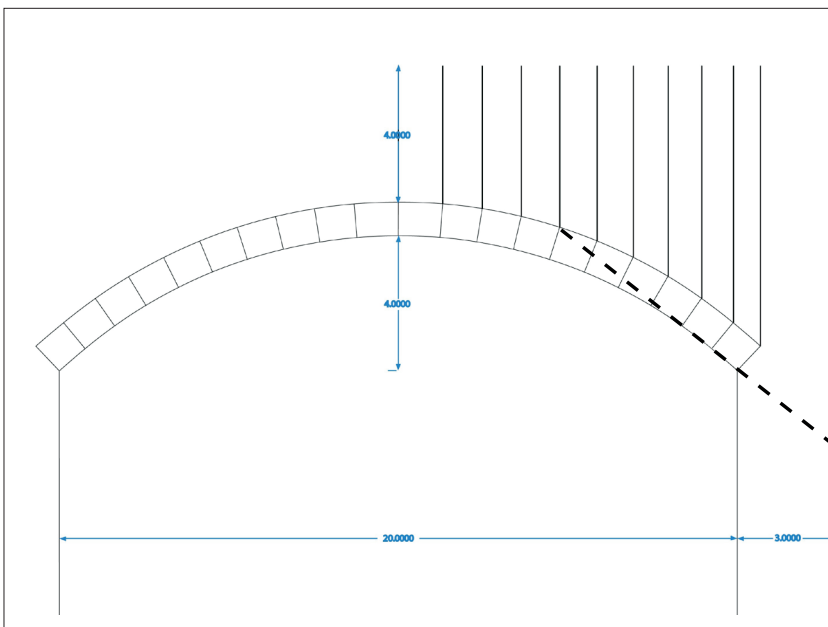
**Combined graphical and plastic analysis.** A modified upper bound on the failure load of the arch is determined by a different graphical method, involving the displacements of an arch at failure. Where the failure of the arch can be identified as the result of forming four hinges, the relative displacement of the three segments between the hinges can be determined by kinematics. A line through a hinge at a fixed support and the first interior hinge intersects a similar line from the other side of the arch at the “instantaneous center” of the displacements in the collapse mechanism. A rotation about the instantaneous center can be imposed on the middle segment, and the relative rotation of the two outside segments can be determined. If the arch and its loads cause negative virtual work in any such mechanism, then the arch can be identified as unstable. The virtual work that results from these displacements is more easily found by drawing a diagram and scaling.

### Example of an Assessment of a Masonry Arch

The above methods can be applied to the assessment of the brick arch shown in Figure 9. The ring thickness of the arch is three rowlock courses (12 inches). The span is 16 feet, and the rise is 4 feet. The radius of the intrados can be calculated as 10 feet. The abutment at the exterior wall (shown to the right of the arch) is 3 feet wide and 8 feet high. The wall extends 4 feet above the opening. The unit weight of brick masonry at 125 pounds per cubic foot will be taken, and a unit wall thickness of 1 foot will be used.

**Empirical analysis.** This arch has a span:rise ratio of 4 and has a span:thickness ratio of 16. The

**Fig. 9.** Diagram of the dimensions of the brick arch in the design example. Figure by Karissa Shaner.



abutment height:width ratio is 8 feet:3 feet = 2.67. Both the span:thickness ratio and the abutment height:width ratio are too large to allow us to rely exclusively on empirical criteria. The dashed line traced on Figure 9 also shows that the abutment width does not satisfy the empirical rule, suggesting that a more detailed assessment of the abutment is necessary.

**Analytical elastic analysis.** The arch has been divided into 20 equal segments and entered into the frame-analysis program SAP2000. The following properties have been entered for each segment: area = 140 in<sup>2</sup>; moment of inertia = 1,730 in<sup>4</sup>; elastic modulus = 1,500,000 lb/in<sup>2</sup>; and compressive strength = 200 lb/in<sup>2</sup>.

The base of the arch at each abutment is fixed.

The load on each of the 10 segments of the half-arch is the sum of the arch segment: 120 pounds for a 1-foot thickness of wall and arch and a section of wall extending through the spandrel to 4 feet above the crown of the arch.

A vertical support reaction of 9.1 kips and a horizontal support reaction of 7.8 kips are calculated by the computer program. Typical bending-moment diagrams output by the computer program are shown in Figure 10. These results are plotted within a failure envelope for brick masonry in Figure 6. The eccentricity values of the axial force do not exceed 3 inches, indicating a stable arch ring. However, the support reaction has a horizontal component of approximately 80 percent of the vertical reaction. A 3-foot-wide, 8-foot-tall abutment on its own is not capable of resisting the overturning moment due to a horizontal reaction of this magnitude, so the abutment would require remedial action.

**Graphical and elastic analysis.** A graphical analysis of the arch is shown in Figure 1. The process of constructing this thrust line consists in assigning a weight to each of the 20 segments of the arch and drawing a vertical load line representing the weight of each of these segments. An arbitrary location for the pole is selected, and the sagging thrust line visible in Figure 1 is constructed (cyan). The first and last strings of this thrust line, extended, represent the crown thrust and the support reaction (green). Extending these two strings to their point of intersection locates the resultant of the loads on the right half of the symmetric arch. Following the construction described above, it is possible to find a thrust line, horizontal at the crown and inclined at the support reaction (magenta). This final thrust line is associated with a pole at the location designated “final choice of pole” on the figure: This thrust line is entirely contained within the arch, representing a

stable structure. It is also possible to begin with a pole location on the horizontal line in the force diagram and to construct the corresponding thrust line by trial and error, relocating the pole as necessary.

This result can be viewed from an elastic or a plastic perspective. Based on elastic analysis, it is possible to determine the total internal thrust at each section of the arch and the eccentricity of the thrust. From there, the maximum elastic stress in the arch can be calculated at every point and compared to an allowable value.

**Graphical and plastic analysis.** The graphical upper-bound analysis is described in Figure 11. Hinges are considered at the abutments and two points within the arch ring. The arch is divided into two sections, at the point where there is an extrados hinge. An instantaneous center of rotation is found by intersecting two lines from fixed points through the adjacent hinges. The negative virtual work (downwards) and positive virtual work (upwards) associated with the rotation about the instantaneous center are found.

**Table 1. Computed Weights of Spandrel Segments.**

Spandrel	Wall area in square feet	Weight in pounds
1	6.33	760
2	6.73	808
3	6.43	771
4	6.11	733
5	5.78	694
6	5.47	656
7	5.20	624
8	4.98	600
9	4.82	578
10	4.70	564

A net-negative virtual work is associated with instability of the arch. To complete the upper-bound analysis shown in Figure 11, different locations of the intrados hinge were chosen. In most hinge locations, positive virtual work resulted from rotation about the instantaneous center. In the case shown, the positive work is 64.9 ft<sup>2</sup>(120 lb/ft<sup>2</sup>)(0.1287ft), and the negative work is 91.2 ft<sup>2</sup>(120 lb/ft<sup>2</sup>)(-0.1204 ft). This reflects the previously established fact that the combination of the segmental arch and limited abutment width results in an unstable structure.

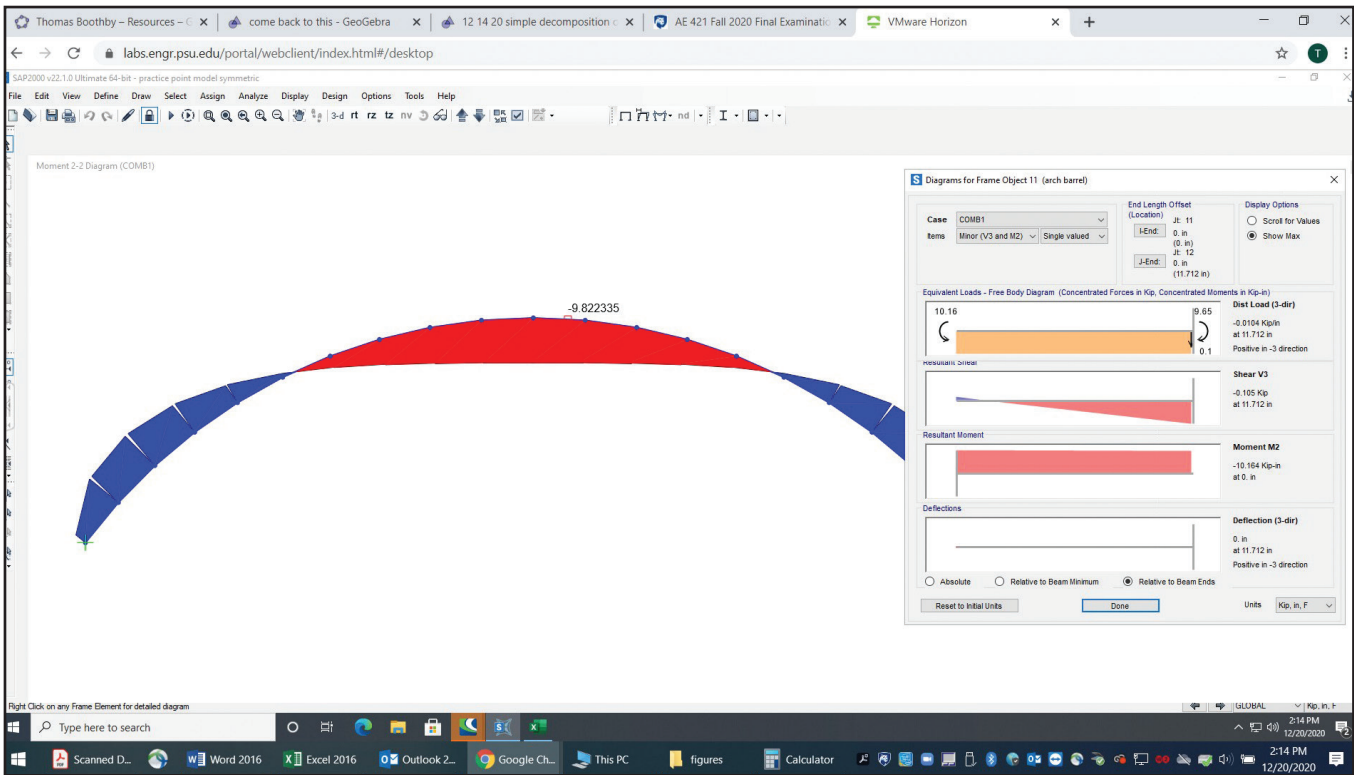


**Fig. 10.**  
A design example of SAP output from frame analysis. This illustration shows the bending-moment diagram for a low-rise segmental arch subjected to loading from the masonry above.

## Conclusions

The preservation engineer can arrive at a reasonable assessment of a brick or stone arch by applying general engineering principles to the specific problem of determining the capacity of an arch.

It is possible to rule out almost immediately a number of issues with a masonry arch by starting with the empirical formulas available for the ratios of an arch structure. Any arch conforming to the given empirical rules is unlikely to fail without the involvement of the abutments or support settlement. The two issues of abutment yielding and support settlement are the most likely causes of failure of any arch system. The flatter the arch, the more susceptible it is to these types of failure.

The arch itself can be assessed by a number of analytical procedures, or it can be studied graphically. General-purpose, elastic frame-analysis programs are suitable for the analysis of an arch structure, provided that the loading and support conditions and the general material properties of the arch are entered correctly. In the example above, all of the methods employed yielded approximately the same conclusion—that the arch itself is adequate but that the width of the abutment threatens instability. This

agreement among the methods is surely not the case in all practical situations. The merit of having a variety of methods available is that the results of one analysis can be checked against the results of another. There appears to be no single method that is better for the preservation engineer, and in the end, the choice of methods to use is a matter of user preference. Engineers who are more comfortable with computer programs will probably prefer to use a computer implementation of an elastic method. Although the application of graphical analysis requires some investment in learning how to use it comfortably, it is a more revealing method for the analysis of arches, as it enables immediate visualization of the thrust line. A number of textbooks describe the use of graphical methods in a more expansive manner than is possible in this *Practice Point*.<sup>12</sup> At the very least, this method can be used as an opportunity to check another form of analysis.

**Thomas E. Boothby** is a professor of architectural engineering at The Pennsylvania State University. He has worked with masonry arches as features of bridges and buildings for the past 30 years. He is the author of *Engineering Iron and Stone* (Washington, D.C.: ASCE Press, 2015). He can be reached at [teb2@psu.edu](mailto:teb2@psu.edu).

## Notes

1. Thomas Boothby, *Engineering Iron and Stone* (Washington, D.C.: ASCE Press, 2015), 26.
2. Thomas Boothby, *Empirical Structural Design for Architects, Engineers, and Builders* (London: ICE Publishing, 2018), 10. Many earlier authors have advanced empirical rules for proportioning arches, including Leonbattista Alberti, *Della Architettura Libri X*, vol. 1 (London: Thomas Edlin, 1739), 17, who recommended that semicircular arches in buildings have a span:thickness ratio of 14. William Rankine, *A Manual of Civil Engineering*, 4th ed. (London: C. Griffin, 1865) presents an empirical ratio for arch bridges based solely on the intrados radius.
3. An empirical rule is given in Boothby based on a geometrical construction; Boothby, *Empirical Structural Design for Architects, Engineers, and Builders*, 11.
4. Ira O. Baker, *A Treatise on Masonry Construction*, 8th ed. (New York: J. Wiley and Sons, 1893), 188.
5. See note 4 for Baker's viewpoint on the position of the thrust line in a stable arch. Jacques Heyman, "The Stone Skeleton," *International Journal of Solids and Structures* 22, no. 2 (1966): 249–279.
6. "Lintel Loading Method: Overview of BS 5977," Stressline, accessed Dec. 12, 2020, <https://www.stressline.net/lintel-loading-method-overview-of-bs-5977/>.
7. Thomas Boothby, "Load Rating of Masonry Arch Bridges," *Journal of Bridge Engineering* 6, no. 2 (April 2001): 79.
8. "Lintel Loading Method: Overview of BS 5977."
9. John. A. Ochsendorf, José. I. Hernando, and Santiago Huerta, "Collapse of Masonry Buttresses," *Journal of Architectural Engineering* 10, no. 3 (Sept. 2004): 88–97.
10. This approach is based on graphic statics, as first compiled by Karl Culmann, *Die Graphische Statik* (Zurich: Meyer und Zeller, 1866). Later refinements specific to the masonry arch were introduced by George Fillmore Swain, *Structural Engineering: Stresses, Graphical Statics, and Masonry*, vol. 3 (New York: McGraw Hill Book Co., 1927); and Frank Kidder, *The Architect's and Engineer's Pocket Book*, 3rd ed. (New York: John Wiley and Sons, 1886).
11. Kidder.
12. One of the easiest introductory books on graphical analysis to follow is Waclaw Zalewski and Edward Allen, *Shaping Structures: Statics* (New York: Wiley, 1988). Readers desiring more depth can consult William Wolfe, *Graphical Analysis* (New York: McGraw Hill Book Co., 1921) or Swain. Other than Zalewski and Allen, all of the above books are available through the HathiTrust website.

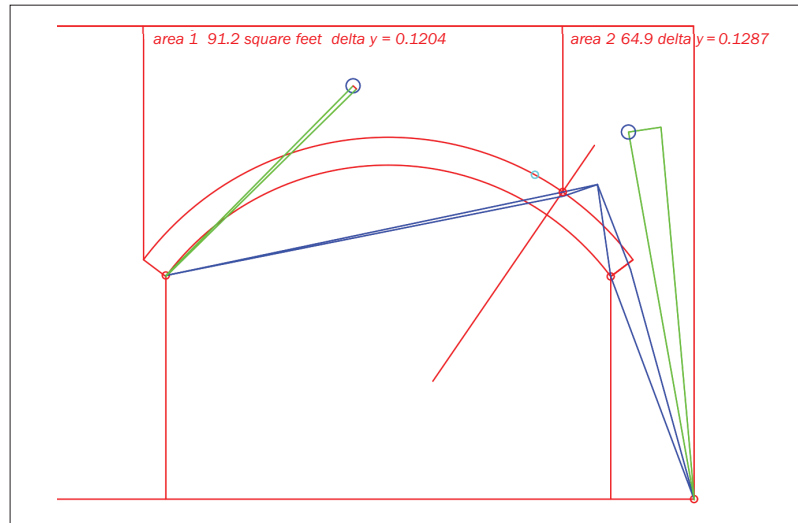


**Fig. 11.**

*Kinematic or upper-bound analysis of the example arch-analysis problem. The arch will collapse by rotation of the weaker abutment about the point shown in its base and by the formation of an intrados hinge at each abutment. The rotation of the two sections of the arch about the instantaneous center (point of convergence of blue lines) defines this collapse mechanism. The virtual work of gravity on the segment to the left opposed to the lifting of the section to the right is assessed: Negative virtual work is associated with instability. Figure by Karissa Shaner.*

© 2021 by the Association for Preservation Technology International. This *Practice Point* originally appeared in Vol. LII, No. 2–3, of the *APT Bulletin: The Journal of Preservation Technology*. Reprint requests should be submitted in writing to the Association for Preservation Technology International.

APT's mission is to advance appropriate traditional and new technologies to care for, protect, and promote the longevity of the built environment and to cultivate the exchange of knowledge throughout the international community.



**The Association for Preservation Technology International**  
 PO Box 7317  
 Springfield, IL 62791  
 217.529.9039

fax 217.529.9120  
 info@apti.org  
 www.apti.org